



HAL
open science

Hepatitis E Virus (HEV) Open Reading Frame 2 Antigen Kinetics in Human-Liver Chimeric Mice and Its Impact on HEV Diagnosis

Ibrahim M Sayed, Lieven Verhoye, Claire Montpellier, Florence
Legrand-Abravanel, Laurence Cocquerel, Philip Meuleman, Jacques Izopet

► **To cite this version:**

Ibrahim M Sayed, Lieven Verhoye, Claire Montpellier, Florence Legrand-Abravanel, Laurence Cocquerel, et al.. Hepatitis E Virus (HEV) Open Reading Frame 2 Antigen Kinetics in Human-Liver Chimeric Mice and Its Impact on HEV Diagnosis. *Journal of Infectious Diseases*, In press, 220 (5), pp.811-819. 10.1093/infdis/jiz171 . hal-02117796

HAL Id: hal-02117796

<https://hal.science/hal-02117796>

Submitted on 2 May 2019

HAL is a multi-disciplinary open access archive for the deposit and dissemination of scientific research documents, whether they are published or not. The documents may come from teaching and research institutions in France or abroad, or from public or private research centers.

L'archive ouverte pluridisciplinaire **HAL**, est destinée au dépôt et à la diffusion de documents scientifiques de niveau recherche, publiés ou non, émanant des établissements d'enseignement et de recherche français ou étrangers, des laboratoires publics ou privés.

24 **Abstract (Word Count= 200)**

25 **Background:** Hepatitis E virus infection (HEV) is an emerging problem in developed countries.

26 Diagnosis of HEV infection is based on the detection of HEV-specific antibodies, viral RNA and/or
27 antigens (Ag). Humanized mice were previously reported as a model for the study of HEV infection,
28 but published data was focused on the quantification of viral RNA. However, the kinetics of HEV Ag
29 expression during the course of infection remains poorly understood.

30 **Methods:** Plasma and fecal suspensions from HEV infected and ribavirin-treated humanized mice
31 were analyzed using HEV antigen ELISA, RT-qPCR, density gradient and Western blotting.

32 **Result:** ORF2 Ag was detected in both plasma and stool of HEV infected mice, and increased over
33 time. Contrary to HEV RNA, ORF2 Ag levels were higher in mouse plasma than in stool. Interestingly,
34 ORF2 was detected in plasma of mice that were RNA negative in plasma but RNA positive in stool;
35 and after viral clearance by ribavirin. Plasma density gradient analysis revealed the presence of the
36 non-infectious glycosylated form of ORF2.

37 **Conclusion:** ORF2 Ag can be used as a marker of active HEV infection and the assessment of antiviral
38 therapy, especially when fecal samples are not available or molecular diagnostic tests are not
39 accessible.

40

41 **Key words:** HEV Ag, humanized mice, ORF2, diagnosis, ribavirin therapy

42

43

44 Introduction

45 Hepatitis E virus (HEV) causes about 20 million infection annually[1]. HEV is a positive sense single
46 stranded RNA virus that belongs to the *Hepeviridae* family, comprising *Orthohepevirus* and
47 *Pescihepevirus* genera. The *Orthohepevirus A* species includes at least 7 genotypes (gt), 5 of which
48 were shown to be capable of causing infection in humans[2, 3]. HEV gt1 and gt2 isolates infect
49 humans only and are dominant in developing countries, while gt3 and gt4 isolates are zoonotic and
50 are more common in industrialized countries[4]. HEV isolates of gt5 and gt6 have been isolated from
51 wild boar in Japan and seem not infectious to humans[5]. HEV gt7 was isolated from camels in the
52 Middle East[6]. To our knowledge, only one human case was diagnosed with camelid HEV
53 infection[7]. More recently, a potential 8th genotype was identified in Bactrian camels in China[8].

54 There are four major routes of HEV transmission: fecal-oral, food borne, blood transfusion and
55 vertical transmission from infected mothers to their babies[1, 4]. Although a typical HEV infection
56 will resolve spontaneously, chronicity, defined by the presence of HEV RNA for at least 3 months, has
57 been observed in immunocompromised patients[9]. Ribavirin (RBV) is the drug of choice for
58 treatment of chronic HEV infection[10, 11].

59 The HEV genome encodes three open reading frames (ORFs), namely ORF1, ORF2 and ORF3. ORF1
60 encodes a non-structural polyprotein that is essential for viral replication. ORF2 encodes the viral
61 capsid protein and is the most immunogenic viral protein. ORF3 encodes a small phosphoprotein
62 that is involved in virion morphogenesis and egress [1, 4]

63 The diagnosis of HEV infection is based mainly on the detection of HEV RNA (gold standard) and/or
64 detection of anti-HEV antibodies (IgM and/or IgG)[12]. Recently, a novel diagnostic assay became
65 commercially available (Beijing Wantai Biological Pharmaceutical Co., Beijing, China), which is based
66 on the detection of HEV ORF2 antigen (Ag). Previous studies showed that this HEV Ag ELISA could be
67 used as a diagnostic tool in clinical laboratories where molecular assays are lacking[13-16]. *Behrendt*
68 *et al.* showed that the sensitivity of the HEV Ag ELISA assay is less than RT-qPCR, especially during

69 acute HEV infection, and that higher HEV Ag levels were detected in chronically infected patients
70 compared to acute ones[17]. They also reported that HEV Ag was detectable for more than 100 days
71 after HEV RNA clearance in ribavirin treated patient[17]. Moreover, *Marion et al.*, recently reported
72 that the serum level of HEV Ag at the acute phase of HEV infection in immunocompromised patients
73 could predict the possibility of HEV chronicity in these patient [18]. Using an HEV cell culture system,
74 *Montpellier et al.*, recently showed that HEV produces 3 different forms of ORF2:
75 infectious/intracellular ORF2 (ORF2i), glycosylated ORF2 (ORF2g) and cleaved ORF2 (ORF2c). The
76 ORF2i protein (80KDa) is the structural component of infectious viral particles and is not
77 glycosylated. In contrast, ORF2g (90KDa) and ORF2c (75KDa) proteins are glycosylated forms that are
78 secreted in large amounts in culture supernatant and are not associated with infectious virions.
79 ORF2g and ORF2c do not form particulate material but, importantly, are the most abundant antigens
80 detected in patient sera [19]. Recently, *Yin et al.* reported that the glycosylated secreted form of
81 ORF2 resembles the virus capsid, but lacks the antigenic epitope predicated to bind the cell receptor
82 [20].

83 Recently, our group and others have established human-liver chimeric mice as a small animal model
84 for the study of HEV infection and the evaluation of novel antiviral therapies[21-26]. Similar to
85 immunocompromised patients, these immunodeficient mice (SCID or Rag-2^{-/-}-IL-2R γ ^{-/-}) develop
86 chronic HEV infection when challenged with different HEV preparations of gt1 and gt3 [21-24]. While
87 HEV infection was confirmed in these models by the detection and quantification of HEV RNA in
88 mouse stool, plasma, bile and liver tissue, the kinetics and characteristics of HEV antigen expression
89 during the course of infection remained unclear.

90 In this study, we characterized the ORF2 antigen secretion during the course of HEV infection in
91 humanized mice and investigated its potential use as marker for antiviral therapy.

92

93

94 **Material and Methods**

95 **1-Production, infection and therapy of human liver chimeric mice**

96 uPA^{+/+}-SCID and FRG mice were transplanted with primary human hepatocytes as previously
97 described[21, 23, 27]. Humanized mice were inoculated intrasplenically or orally with fecal
98 suspensions or plasma containing HEV of gt1 or gt3. Plasma and fecal samples were regularly
99 collected from the inoculated mice and stored at -80°C until analysis. Ribavirin (RBV) treatment was
100 performed at 50 mg/kg as previously described [21]. Details on the pharmacokinetic analysis of HEV
101 ORF2 antigen in non-humanized mice are described in the supplemental materials and methods
102 section. All procedures were performed according to European and Belgian legislation; and were
103 approved by the Animal Ethics Committee of the Faculty of Medicine and Health Sciences of Ghent
104 University.

105 **2-Detection and quantification of HEV RNA in mouse samples**

106 Viral RNA was extracted from 10% (w/v) mouse fecal preparations and mouse plasma using the
107 NucliSENS easyMAG system (Biomérieux, France). HEV RNA was detected and quantified using
108 primers targeting HEV ORF3 as described previously[21]. Nested PCR using primers targeting HEV
109 ORF2 was performed on mouse samples with low viral load as described previously[23].

110 **3-Detection of HEV Ag in mouse samples**

111 Detection of HEV Ag in mouse samples was performed using the HEV-Ag ELISA^{Plus} assay (Beijing
112 Wantai Biological Pharmaceutical Co., China) according to the manufacturer's instructions, with
113 slight modifications to determine the cut-off (C.O.), as described in the supplementary material and
114 methods section.

115 **4-Density gradient analysis**

116 Mouse plasma and 10% (w/v) mouse stool suspensions were prepared from HEV-infected and non-
117 infected mice, and were ultra-centrifuged as previously described[21]. More details are available in
118 the supplementary material and methods section

119

120 **5- Statistic analyses**

121 The geometric mean of the viral load and HEV Ag level was determined in mouse samples at the
122 start of RBV therapy and EOT. Statistical significance was calculated by GraphPad Prism version 6.1
123 using a paired two-tailed Student's t-test.

124 **Results**

125 **1- Kinetic analysis of HEV Ag secretion in HEV-infected human-liver chimeric mice**

126 Plasma and 10% (w/v) fecal suspensions from HEV infected humanized mice were analyzed for HEV
127 RNA and ORF2 Ag. The HEV RNA data was extensively described in our previous publications [21, 23],
128 but we here correlate the viral RNA levels with the amount of ORF2 antigen present in each sample.
129 In parallel to the HEV RNA load, the level of HEV Ag increased over time in both plasma and 10% w/v
130 fecal preparations of HEV gt1 (Figure 1) and gt3 (Figure 2) infected mice. Similar to the HEV RNA
131 load, the observed HEV Ag levels were considerably higher in HEV gt1-infected mice compared to
132 those in gt3-infected mice (Figure 1 and 2).

133 When comparing the ratio of HEV RNA to HEV ORF2 Ag, we observed an overall inverse relation
134 between the plasma and the feces. Plasma contained relatively higher levels of ORF2 Ag than HEV
135 RNA, while at the corresponding time points the relative level of viral RNA in fecal suspensions was
136 higher than the amount of ORF2 Ag (Figure 1). This indicates that the large amounts of ORF2 Ag
137 present in mouse plasma likely correspond to non-infectious ORF2 Ag, as previously shown for
138 human sera [19].

139 HEV ORF2 Ag levels were very low (near or below cut-off) in mouse stool samples, especially during
140 the early phase of infection where the viral load was already relatively high in most animals (RNA
141 level up to 10^5 - 10^6 IU/ml)(Figure 1 and 2). In one mouse, the viral RNA was detectable in stool by RT-
142 qPCR (Figure 2B) starting from week 2 until week 16 post inoculation. However, HEV ORF2 levels
143 remained below cut-off in all tested fecal samples. On the other hand, HEV ORF2 Ag was detected in
144 certain mouse plasma samples in which HEV RNA was under limit of detection (Figure 2A and C),
145 confirming our hypothesis that the non-infectious forms of ORF2 were abundantly present in mouse
146 plasma.

147 As can be seen in Figure 1 and 2, ORF2 levels increased over time, especially in HEV gt1-infected
148 mice, but this increase was not always concomitant with an increase in HEV RNA load. In one mouse
149 (Figure 1C), viremia was nearly stable during the course of infection, but the ORF2 Ag level increased
150 sharply over the same 5-week period. This again suggests that the non infectious forms of ORF2
151 accumulate in the plasma of infected mice.

152 **2- ORF2 status in humanized mice with low HEV replication and in mice after oral HEV challenge.**

153 Next, we examined the HEV ORF2 Ag status in samples obtained from mice with low HEV replication.
154 In these mice, the viral load was under limit of quantification (LOQ) in the plasma during the course
155 of HEV infection, while HEV RNA was continuously detectable in feces but at a relatively low level
156 (2×10^3 to 5×10^4 IU/ml). As shown in Figure 3, HEV ORF2 was not detected in any of the tested
157 plasma and stool samples.

158 Similarly, we evaluated whether HEV ORF2 could be detected in humanized mice that were orally
159 inoculated with multiple HEV preparations. We have previously shown that oral inoculation does not
160 lead to HEV infection and that HEV RNA remains under LOD in the plasma and stool [21, 23]. Here,
161 we detected ORF2 only the first week after inoculation, and only in stool suspensions (Supplemental
162 Figure 1). HEV ORF2 was never detected in any of the subsequent samples.

163 **3- Characterization of HEV ORF2 present in mouse samples**

164 Iodixanol density gradient centrifugation was performed on mouse plasma and 10% (w/v) mouse
165 stool suspensions collected at different time points after viral inoculation to evaluate which of the
166 different ORF2 forms were present. RT-qPCR, HEV ORF2 Ag ELISA and WB analysis were performed
167 on each fraction. We first focused on the analysis of mouse plasma samples collected before and 1, 5
168 and 10 weeks after infection. As shown in Figure 4, the peak of HEV RNA was identified in fraction 6
169 (density 1.11 g/l), while the peak of HEV Ag was always observed in fraction 4 (density 1.09 g/l). One
170 week after viral inoculation, HEV ORF2 was detected by ELISA in fraction 4 and not in the RNA

171 enriched infectious fraction 6. Western blot analysis confirmed the observations made by ELISA and
172 revealed that the ORF2g protein (90 kDa non-infectious glycosylated form) was the only form
173 detectable in plasma.

174 At later time points (week 5 and 10 post-infection), HEV ORF2 Ag became detectable in more density
175 gradient fractions, confirming our previous observation that the secretion of HEV ORF2 Ag is a slow
176 and accumulative process. HEV ORF2 was detected in different mouse plasma fractions which did
177 not contain HEV RNA. Western blot analysis revealed that the ORF2g protein remained the major
178 ORF2 form in mouse plasma at these later time points (Figure 4). We did not detect the infectious
179 ORF2 form (ORF2i) in any of the mouse plasma fractions at any time point.

180 Density gradient analysis of fecal samples revealed that the peak of HEV RNA and HEV ORF2 Ag was
181 found in fraction 10 (1.16 g/l) and fraction 3 (1.07 g/l), respectively (Supplementary Figure 2A). The
182 relative amount of HEV ORF2 Ag was lower in stool fractions compared to plasma fractions, while
183 this was the opposite for the HEV RNA level. Again, HEV ORF2 Ag was not detected by ELISA in the
184 stool infectious fraction (fraction 10). In addition, we did not visualize any form of ORF2 in the stool
185 fractions using Western blotting (data not shown). Unlike the HEV RNA distribution, the distribution
186 of HEV ORF2 Ag among the different stool fractions was similar to the distribution of ORF2 Ag among
187 plasma fractions (Supplementary Figure 2B and C).

188 **4-Kinetics of HEV ORF2 Ag in humanized mice during the course of ribavirin therapy**

189 Five HEV infected humanized mice underwent a 2-week ribavirin (RBV) therapy at 50 mg/kg. HEV
190 ORF2 Ag and HEV RNA were tested both in plasma and 10% (w/v) stool suspensions at 3 different
191 moments: start of therapy (SOT), end of therapy (EOT) and at viral relapse. Similar to the effect on
192 viral RNA load, RBV therapy caused a reduction in the level of ORF2 in both the stool and the plasma
193 of the treated mice (Figure 5). Although, the reduction in viremia was more pronounced than the
194 reduction in fecal RNA load, the reduction of ORF2 in plasma was less than the reduction in fecal
195 ORF2Ag. At the SOT, the geometric mean of fecal RNA load and HEV Ag level in five mice was

196 5.1x10⁶IU/ml and 12.48 A/C.O., respectively, and were reduced at EOT to 2.05x10⁵ IU/ml and 3.75
197 A/C.O., respectively (Figure 5A and B). While the geometric mean of viremia and plasma HEV Ag
198 level in these mice at the start of therapy were 2.95x10⁴IU/ml and 26.1 A/C.O., respectively, and
199 their levels were reduced to the limit of quantification (LOQ=4.05x10² IU/ml) and 14.49 A/C.O.,
200 respectively at EOT (Figure 5A and B). The reduction in the fecal HEV Ag, but not plasma HEV Ag, was
201 statistically significant (P=0.0008) (Figure 5A). Interestingly, the level of HEV Ag was increased again
202 in both the plasma and stool of the treated mice after cessation of therapy (Figure 5C).

203 **5- Assessment of *in vivo* stability of HEV ORF2**

204 In order to evaluate how long ORF2 remains detectable in plasma and feces after secretion from the
205 liver, we inoculated two groups of non-humanized mice with iodixanol cushion-isolated HEV ORF2
206 preparations containing either the three forms of ORF2 (ORF2i, ORF2g and ORF2c), or only the non-
207 infectious form of ORF2 (ORF2g and ORF2c). The amount of HEV RNA and ORF2 protein present in
208 plasma and feces were quantified daily. HEV ORF2 Ag was detectable in mouse stool and plasma
209 samples from both groups, but the level decreased gradually until ORF2disappeared completely
210 within 1 week (Figure 6). HEV RNA was under LOQ in all tested samples.

211

212

213 **Discussion**

214 HEV virus infection is mainly diagnosed by detection of HEV-specific IgM antibodies and/or detection
215 of HEV RNA. A diagnostic ELISA assay based on the detection of HEV ORF2 Ag in patient plasma
216 samples became recently commercially available. The sensitivity and specificity of this assay was
217 reported previously[13-15, 17], and it is recommended in clinical settings where molecular diagnosis
218 is not available. HEV Ag can be used as a diagnostic marker in the window period and in chronic HEV
219 infection, especially in immunocompromised patients in whom seroconversion may be delayed or
220 absent[15, 17, 28, 29].The kinetics of HEV Ag detection during the course of HEV infection is not
221 known. Here, we used human liver chimeric mice (uPA-SCID and FRG background) to study the
222 kinetics of HEV Ag expression during the course of HEV infection and therapy. Since the adaptive
223 immune system is lacking in these mice, chronic HEV infection is developed when these mice are
224 challenged with HEV preparations.

225 HEV Ag was detected in both mouse plasma and stool preparations of HEV infected humanized mice.
226 In addition, the Ag level increased with time suggesting that HEV Ag is a relevant marker of active
227 HEV replication. The level of HEV Ag was higher in mouse samples at later time points of infection,
228 indicating that the production of HEV Ag is cumulative. In a similar manner, *Behrendt et al.* reported
229 that the HEV Ag level can differentiate between acute and chronic HEV infection; i.e. higher HEV Ag
230 levels were detected in chronic HEV infected patients [17]. HEV Ag levels were higher in HEV gt1
231 infected mice than in HEV gt3 infected mice, confirming our previous data showing that HEV gt3 is
232 less virulent than HEV gt1[21]. In contrast to the HEV RNA load, HEV Ag was relatively higher in
233 mouse plasma than in fecal suspensions. In addition, HEV Ag was detected in a few plasma samples
234 that scored negative for HEV RNA, suggesting that detected Ag likely corresponds to non-infectious
235 ORF2 proteins. Our results are in agreement with previous studies that proposed that non-infectious
236 ORF2 proteins are the major antigens in cell culture supernatant and patient sera[19].

237 HEV Ag was not be detected in HEV infected mice which were non-viremic and in which the fecal
238 viral load was relatively low. This is probably due the limited amount of Ag secreted into the plasma
239 that was too low to be detectable by ELISA. Our results suggest that in case low-level HEV replication
240 is expected, qPCR analysis on stool samples is the best option for diagnosis, especially in
241 immunocompromised patients where seroconversion is delayed. Similarly, several groups reported
242 that HEV-Ag ELISA assay is less sensitive than PCR especially when the viral load is low [12, 14, 15,
243 17].

244 Analysis of mouse gradient fractions showed that the peak of HEV Ag is different from the peak of
245 HEV RNA. The peak of HEV RNA in mouse stool sample was 1.16 g/l and the peak of HEV RNA in
246 mouse plasma was 1.11 g/l. This difference may be attributed to the presence of lipids around or
247 associated with the virions that circulate in the plasma [21]. On the other hand, the distribution of
248 HEV Ag in plasma was similar to that in stool. The ORF2g protein was the major ORF2 form detected
249 in mouse plasma. Our results agree with *Montpellier et al.*, who showed that the peak of HEV Ag in
250 patient plasma samples was at 1.08 g/l, and non-infectious ORF2 proteins (ORF2c/ORF2g) were the
251 major Ag present[19]. HEV Ag could be detected in some mouse plasma fractions that were devoid
252 of viral nucleic acid. Similarly, *Behrendt et al.* detected HEV Ag in all gradient fractions of HEV patient
253 sera suggesting the presence of distinct fragments of the viral capsid protein with different
254 densities[17]. The presence of high levels of non-infectious ORF2 in mouse plasma might also explain
255 the low infectivity of plasma preparation compared to stool preparation [21, 23]. The amount of HEV
256 Ag present in mouse stool fraction was relatively low, which impeded its characterization by
257 Western blotting.

258 Next, we tested the effect of RBV therapy on the HEV Ag level in mouse samples. We found that RBV
259 causes a reduction in both the plasma and fecal HEV Ag level, and the reduction was statistically
260 significant in mouse stool samples but not in plasma. In all treated mice, the reduction of HEV Ag
261 was concomitant with the reduction of HEV RNA in mouse stool, while most mice became non-

262 viremic at EOT, HEV Ag remained detectable in mouse plasma. This indicates that viral Ag remains
263 present in mouse plasma even after clearance of infection. Our results agree with *Behrendt et al.*,
264 who reported that HEV Ag could be detected in patient plasma for more than 100 days after HEV
265 clearance. Similarly, prolonged fecal shedding has been shown in patients on RBV therapy, despite
266 undetectable viremia [21, 30, 31].

267 The apparent effect of RBV therapy on HEV infection depends on the viral marker of interest and the
268 compartment analyzed. Our data indicates that in plasma RBV especially has an effect on the
269 secretion of infectious viral particles (HEV RNA) and less on secreted ORF2 that is not associated with
270 RNA. The differential effect on plasma versus fecal RNA suggests that when RBV interferes with viral
271 replication, the available viral RNA is preferentially packaged into particles that are secreted into the
272 bile-canalicular pathway rather than those secreted into plasma. Our results are in agreement with
273 recent data published by *Capelli et al.*, who reported that infectious HEV particles are mainly
274 released to the bile, while only small fractions are released to the blood [32]. Importantly, HEV Ag
275 levels increased after therapy cessation indicating that HEV Ag can be also used as a surrogate
276 marker for HEV relapse.

277 Finally, we assessed the *in vivo* stability of HEV ORF2 in absence of HEV replication, i.e. after
278 injection in non-humanized mice. HEV ORF2 gradually disappeared within 1 week from both feces
279 and plasma, while viral RNA immediately became undetectable. This is faster than what we observed
280 in our RBV treatment study, indicating that during treatment there was remaining low-level viral
281 replication and protein secretion into the plasma. Hence also explaining the presence of HEV RNA
282 and Ag in the mouse stool and relapse after therapy cessation. Although the study by *Behrendt et al.*
283 did not mention any stool data, the persistence of HEV Ag in the patient plasma after RBV therapy
284 must have been due to same reason. Further studies are needed to ascertain this point.

285 In conclusion, our results show the kinetics of HEV Ag during the course of HEV infection, therapy
286 and relapse. The differential impact of RBV therapy on viral RNA and antigen depending on the

287 samples type (feces vs. plasma) is important for the interpretation of HEV diagnosis and evaluation
288 of anti-HEV therapy, especially for laboratories where molecular diagnosis is not available and HEV
289 Ag is the only diagnostic marker available.

290

291

292 **References**

- 293 1. Sayed IM, Vercauter AS, Abdelwahab SF, Vercauteren K, Meuleman P. Is hepatitis E virus an
294 emerging problem in industrialized countries? *Hepatology (Baltimore, Md)* **2015**; 62:1883-92.
- 295 2. Smith DB, Simmonds P, Jameel S, et al. Consensus proposals for classification of the family
296 Hepeviridae. *The Journal of general virology* **2015**; 96:1191-2.
- 297 3. Smith DB, Simmonds P, Izopet J, et al. Proposed reference sequences for hepatitis E virus
298 subtypes. *The Journal of general virology* **2016**; 97:537-42.
- 299 4. Sayed IM, Vercauteren K, Abdelwahab SF, Meuleman P. The emergence of hepatitis E virus in
300 Europe. *Future Virology* **2015**; 10:763-78.
- 301 5. Takahashi M, Nishizawa T, Sato H, et al. Analysis of the full-length genome of a hepatitis E virus
302 isolate obtained from a wild boar in Japan that is classifiable into a novel genotype. *The Journal of*
303 *general virology* **2011**; 92:902-8.
- 304 6. Woo PC, Lau SK, Teng JL, et al. New hepatitis E virus genotype in camels, the Middle East.
305 *Emerging infectious diseases* **2014**; 20:1044-8.
- 306 7. Lee GH, Tan BH, Teo EC, et al. Chronic Infection With Camelid Hepatitis E Virus in a Liver
307 Transplant Recipient Who Regularly Consumes Camel Meat and Milk. *Gastroenterology* **2016**;
308 150:355-7.e3.
- 309 8. Woo PC, Lau SK, Teng JL, et al. New Hepatitis E Virus Genotype in Bactrian Camels, Xinjiang, China,
310 2013. *Emerging infectious diseases* **2016**; 22:2219-21.
- 311 9. Kamar N, Selves J, Mansuy JM, et al. Hepatitis E virus and chronic hepatitis in organ-transplant
312 recipients. *The New England journal of medicine* **2008**; 358:811-7.
- 313 10. Wedemeyer H, Pischke S, Manns MP. Pathogenesis and treatment of hepatitis e virus infection.
314 *Gastroenterology* **2012**; 142:1388-97.e1.
- 315 11. Kamar N, Izopet J, Tripon S, et al. Ribavirin for chronic hepatitis E virus infection in transplant
316 recipients. *The New England journal of medicine* **2014**; 370:1111-20.

- 317 12. Vollmer T, Knabbe C, Dreier J. Comparison of real-time PCR and antigen assays for detection of
318 hepatitis E virus in blood donors. *Journal of clinical microbiology* **2014**; 52:2150-6.
- 319 13. Gupta E, Pandey P, Pandey S, Sharma MK, Sarin SK. Role of hepatitis E virus antigen in confirming
320 active viral replication in patients with acute viral hepatitis E infection. *Journal of clinical virology :*
321 *the official publication of the Pan American Society for Clinical Virology* **2013**; 58:374-7.
- 322 14. Tremeaux P, Lhomme S, Chapuy-Regaud S, et al. Performance of an antigen assay for diagnosing
323 acute hepatitis E virus genotype 3 infection. *Journal of clinical virology : the official publication of the*
324 *Pan American Society for Clinical Virology* **2016**; 79:1-5.
- 325 15. Zhao C, Geng Y, Harrison TJ, Huang W, Song A, Wang Y. Evaluation of an antigen-capture EIA for
326 the diagnosis of hepatitis E virus infection. *Journal of viral hepatitis* **2015**; 22:957-63.
- 327 16. Sayed IM, Vercouter AS, Meuleman P. Hepatitis E virus in acute liver failure: An unusual suspect?
328 *Hepatology (Baltimore, Md)* **2016**; 64:1837-9.
- 329 17. Behrendt P, Bremer B, Todt D, et al. Hepatitis E Virus (HEV) ORF2 Antigen Levels Differentiate
330 Between Acute and Chronic HEV Infection. *The Journal of infectious diseases* **2016**; 214:361-8.
- 331 18. Marion O, Capelli N, Lhomme S, et al. Hepatitis E virus genotype 3 and capsid protein in the
332 blood and urine of immunocompromised patients. *The Journal of infection* **2019**.
- 333 19. Montpellier C, Wychowski C, Sayed IM, et al. Hepatitis E Virus Lifecycle and Identification of 3
334 Forms of the ORF2 Capsid Protein. *Gastroenterology* **2018**; 154:211-23.e8.
- 335 20. Yin X, Ying D, Lhomme S, et al. Origin, antigenicity, and function of a secreted form of ORF2 in
336 hepatitis E virus infection. *Proceedings of the National Academy of Sciences of the United States of*
337 *America* **2018**; 115:4773-8.
- 338 21. Sayed IM, Verhoye L, Cocquerel L, et al. Study of hepatitis E virus infection of genotype 1 and 3 in
339 mice with humanised liver. *Gut* **2017**; 66:920-9.
- 340 22. Allweiss L, Gass S, Giersch K, et al. Human liver chimeric mice as a new model of chronic hepatitis
341 E virus infection and preclinical drug evaluation. *Journal of hepatology* **2016**; 64:1033-40.

342 23. Sayed IM, Foquet L, Verhoye L, et al. Transmission of hepatitis E virus infection to human-liver
343 chimeric FRG mice using patient plasma. *Antiviral research* **2017**; 141:150-4.

344 24. van de Garde MD, Pas SD, van der Net G, et al. Hepatitis E Virus (HEV) Genotype 3 Infection of
345 Human Liver Chimeric Mice as a Model for Chronic HEV Infection. *Journal of virology* **2016**; 90:4394-
346 401.

347 25. Sayed IM, Meuleman P. Murine Tissues of Human Liver Chimeric Mice Are Not Susceptible to
348 Hepatitis E Virus Genotypes 1 and 3. *The Journal of infectious diseases* **2017**; 216:919-20.

349 26. Todt D, Moeller N, Praditya D, et al. The natural compound silvestrol inhibits hepatitis E virus
350 (HEV) replication in vitro and in vivo. *Antiviral research* **2018**; 157:151-8.

351 27. Meuleman P, Libbrecht L, De Vos R, et al. Morphological and biochemical characterization of a
352 human liver in a uPA-SCID mouse chimera. *Hepatology (Baltimore, Md)* **2005**; 41:847-56.

353 28. Zhang F, Li X, Li Z, et al. Detection of HEV antigen as a novel marker for the diagnosis of hepatitis
354 E. *Journal of medical virology* **2006**; 78:1441-8.

355 29. Majumdar M, Singh MP, Pujhari SK, Bhatia D, Chawla Y, Ratho RK. Hepatitis E virus antigen
356 detection as an early diagnostic marker: report from India. *Journal of medical virology* **2013**; 85:823-
357 7.

358 30. Abravanel F, Lhomme S, Rostaing L, Kamar N, Izopet J. Protracted fecal shedding of HEV during
359 ribavirin therapy predicts treatment relapse. *Clinical infectious diseases : an official publication of*
360 *the Infectious Diseases Society of America* **2015**; 60:96-9.

361 31. Ambrosioni J, Mamin A, Hadengue A, et al. Long-term hepatitis E viral load kinetics in an
362 immunocompromised patient treated with ribavirin. *Clinical microbiology and infection : the official*
363 *publication of the European Society of Clinical Microbiology and Infectious Diseases* **2014**; 20:O718-
364 20.

365 32. Capelli N, Marion O, Dubois M, et al. Vectorial Release of Hepatitis E Virus in Polarized Human
366 Hepatocytes. *Journal of virology* **2018**.

367

368

369

370

371 **Author contributions:** IMS, CM, LC and PM designed the experiments. IMS, LV and CM performed
372 experiments. IMS, LC, , CM and PM analyzed data. FA and JI provided essential reagents. IMS and PM
373 wrote the manuscript. PM conceived and supervised the study.

374

375 **Funding** This study was funded by the Ghent University and the Lille 2 University (IRO project
376 MODEL-HEPE), The Research Foundation—Flanders (FWO-Vlaanderen; projects G0D2715N,
377 G047417N and EOS project VirEOS30981113), the Agency for Innovation by Science and Technology
378 (IWT SBO project HLIM-3D), and the ‘Agence Nationale de Recherches sur le Sida et les hépatites
379 virales’ (ANRS). IMS is a recipient of a PhD fellowship provided by the Egyptian Government and
380 Ghent University.

381

382 **Competing interests** None.

383

384

385

386

387

388

389

390

391
 392
 393
 394
 395
 396
 397
 398
 399
 400
 401
 402
 403
 404
 405
 406
 407
 408
 409
 410
 411
 412

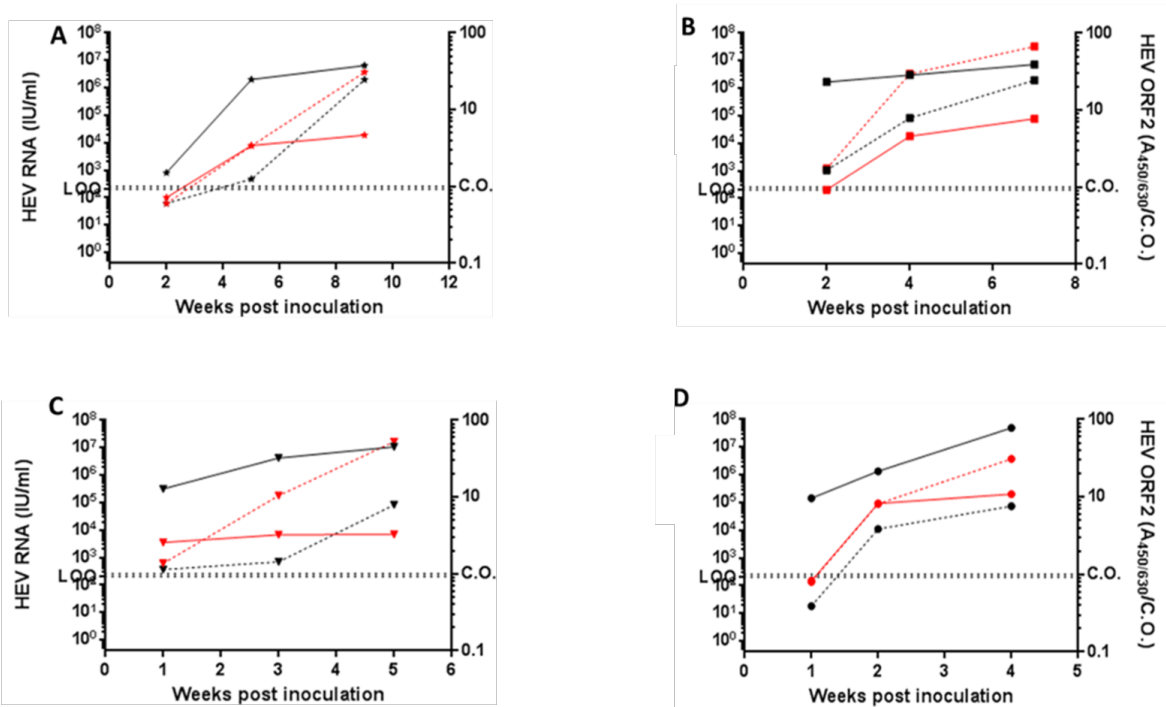


Figure 1: Evolution of HEV ORF2 and viral RNA in genotype 1 (gt1) HEV-infected humanized mice.

Humanized mice (n=4) were inoculated with HEV of gt1 (SAR-55 strain). HEV RNA (solid line; IU/ml, left Y-axis) and HEV ORF2 (dotted line; $A_{450/630}/C.O.$, right axis) were measured at different time points after inoculation in both mouse plasma (red) and feces (black). LOQ: limit of quantification. C.O.: cut-off. Each panel (A, B, C and D) represents data from individual mice.

413
414
415
416
417
418
419
420
421
422
423
424
425
426
427
428
429
430
431
432

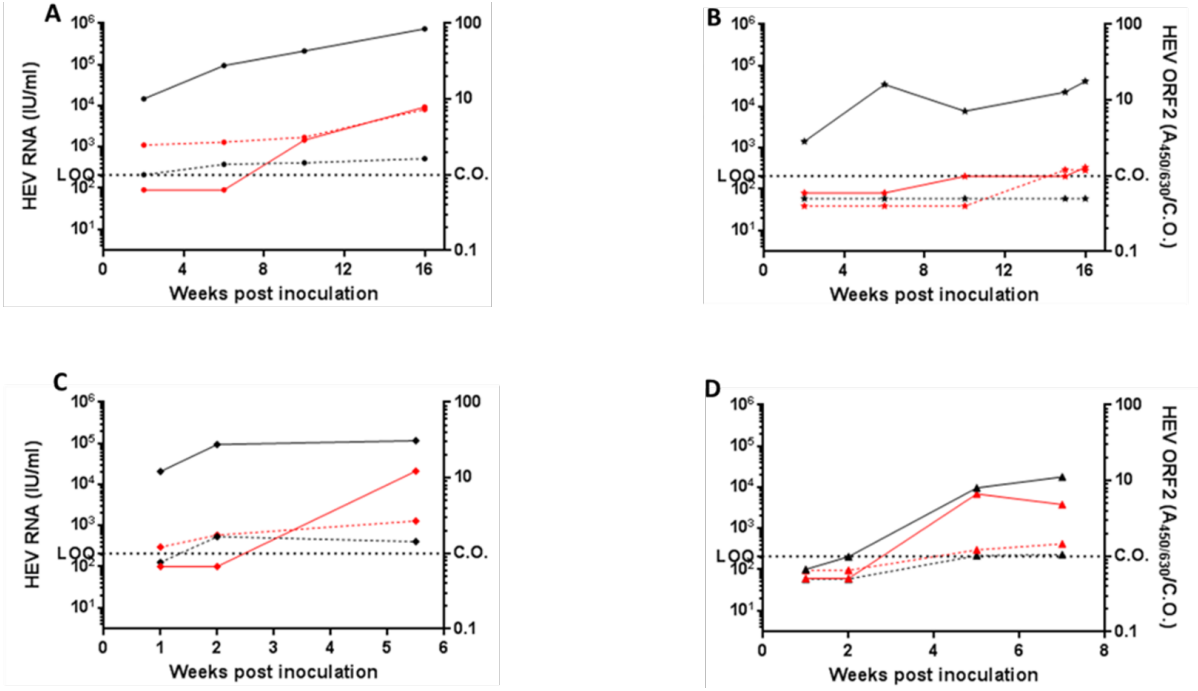
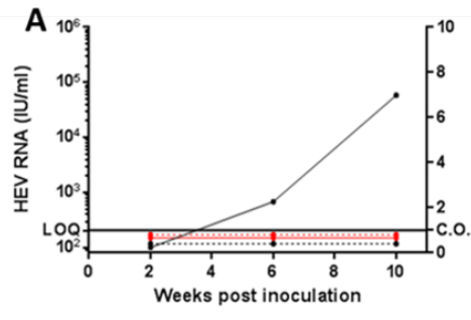


Figure 2: Evolution of HEV ORF2 and viral RNA in genotype 3 (gt3)HEV-infected humanized mice.

Humanized mice (n=4) were inoculated with an HEV patient isolate of gt3. HEV RNA (solid line; IU/ml, left Y-axis) and HEV ORF2 (dotted line; A_{450/630}/C.O., right axis) were measured at different time points after inoculation in both mouse plasma (red) and feces (black). LOQ: limit of quantification. C.O.: cut-off. Each panel (A, B, C and D) represents data from individual mice.

433

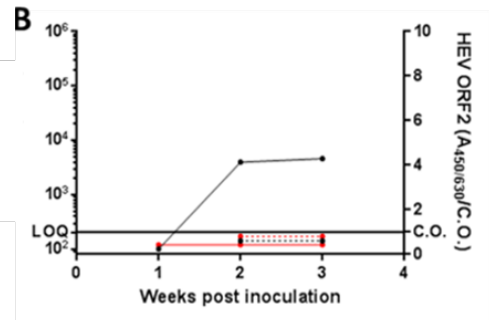


434

435

436

437

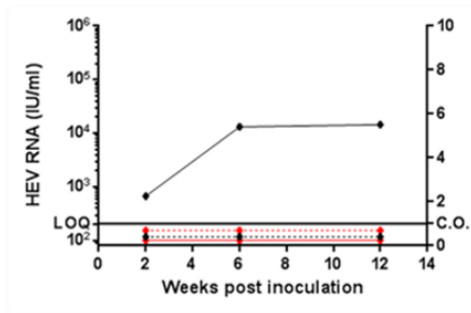


438

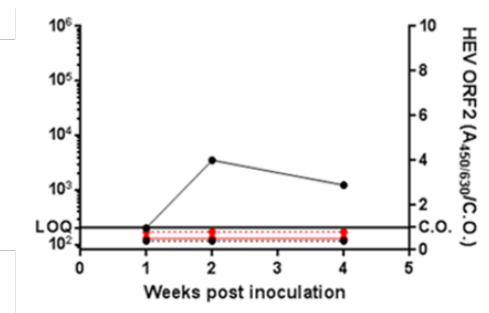
439

440

441



442

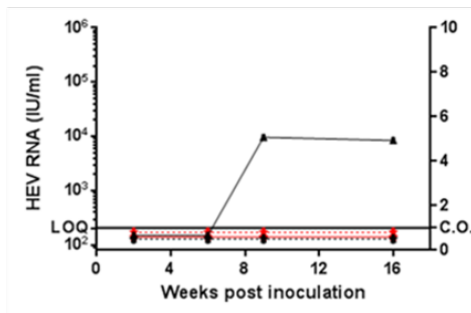


443

444

445

446



447

448 **Figure 3: Absence of HEV ORF2 Ag in humanized mice with low HEV replication.** Humanized mice

449 were inoculated with HEV of gt3 (panel A, n=3) or HEV of gt1 (panel B, n=2). Viral RNA (solid line;

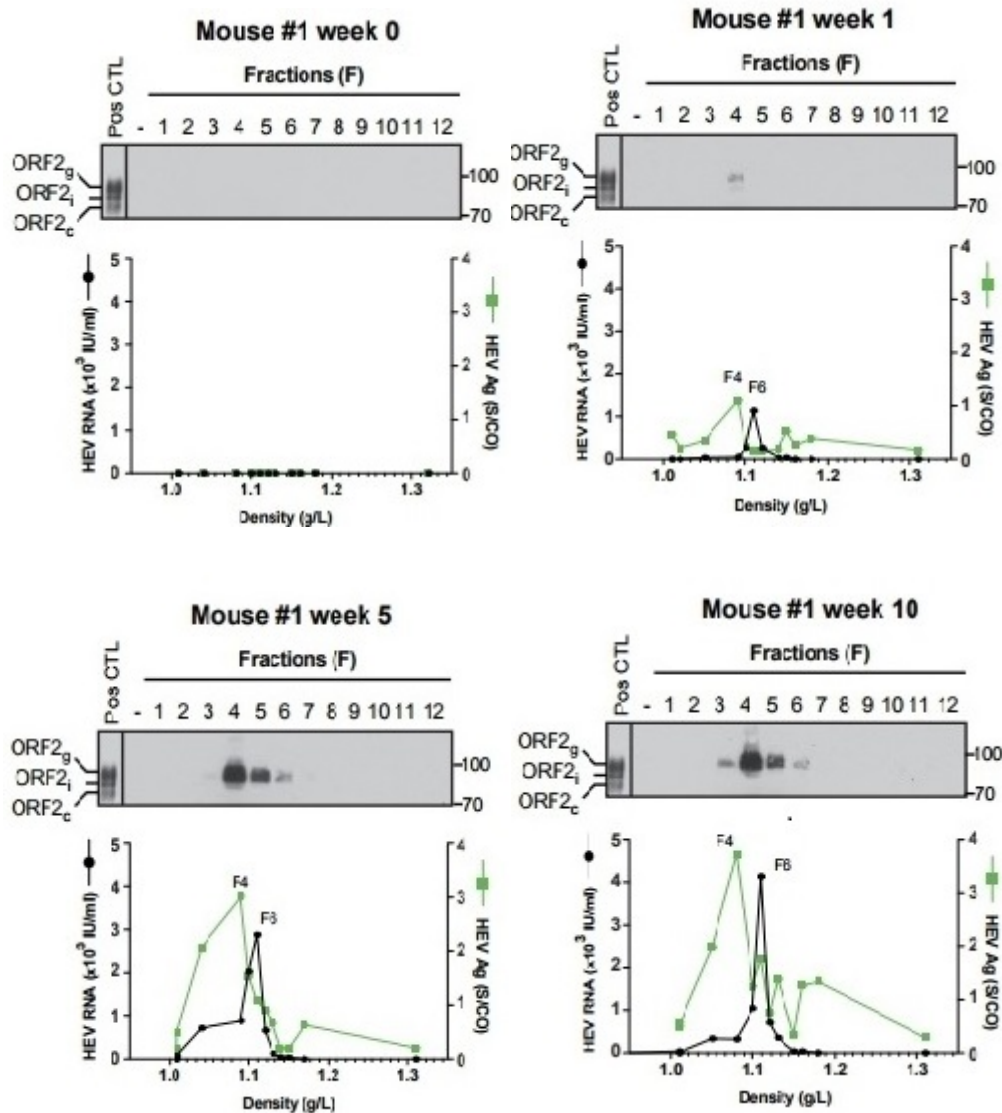
450 IU/ml, left Y-axis) and ORF2 protein (dotted line; A_{450/630}/C.O., right axis) were measured at different

451 time points after inoculation. Black lines represent data obtained from mouse stool, while red lines

452 represent data obtained from mouse plasma analyses. LOQ: limit of quantification. C.O.: cut-off.

453

454



455

456

457 **Figure 4: Mouse plasma density gradient analysis during the course of HEV infection.**

458 Plasma collected before HEV infection (week 0) and at different time points post infection (week 1, 5

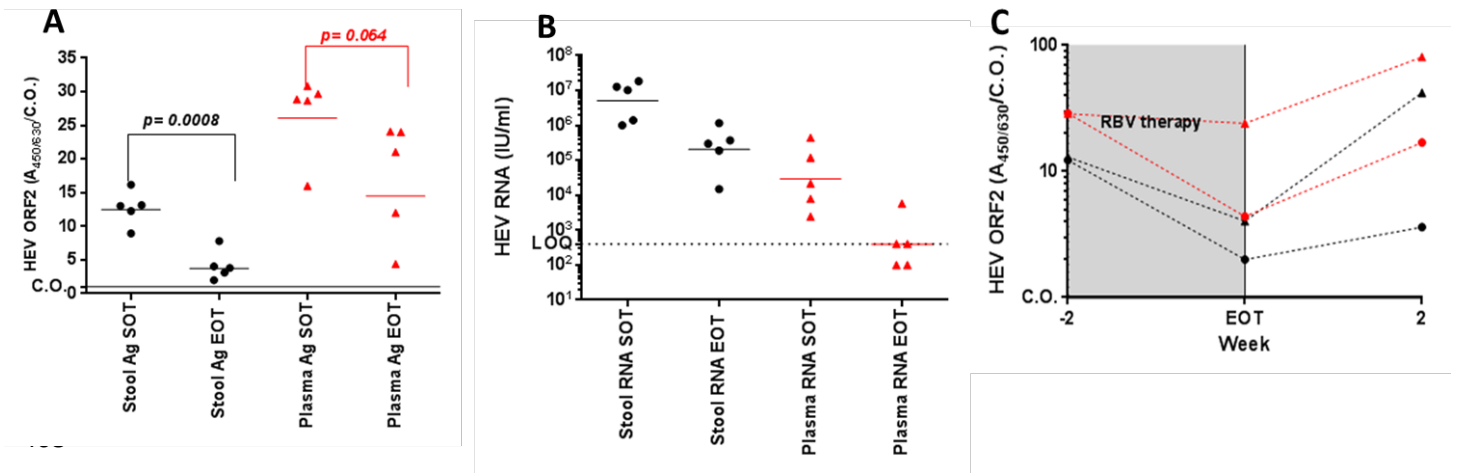
459 and 10) was processed by iodixanol density gradient ultracentrifugation and the gradient fractions

460 were analyzed by Western blotting, ORF2-specific ELISA and RT-qPCR. HEV RNA levels (left Y-axis) are

461 represented by black lines, while HEV ORF2 Ag levels are shown in green.

462

463

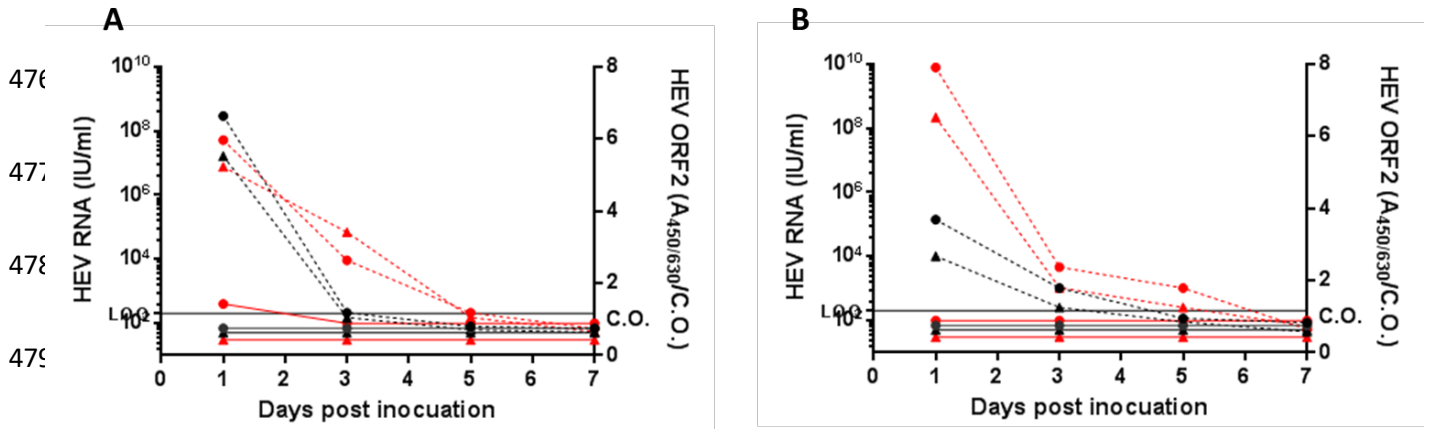


469 **Figure 5: Kinetics of HEV Ag during ribavirin therapy in humanized mice.**

470 Humanized mice (n=5) were treated orally with RBV for 2 weeks. HEV Ag (A) and HEV RNA (B) were
 471 measured at start (SOT) and end of therapy (EOT). HEV Ag was monitored in two humanized after
 472 RBV therapy cessation (C). Fecal and plasma data are shown in black and red respectively. Horizontal
 473 lines represent the geometric mean. LOQ: is limit of quantification.

474

475



480

481 **Figure 6: Evaluation of HEV ORF2 stability in non-humanized mice.** Non-transplanted mice (n=4)
 482 were inoculated with a preparation containing the 3 known forms of ORF2 (panel A; n=2) or a
 483 preparation only containing the non-infectious form of ORF2 (panel B; n=2). HEV RNA (solid line) and
 484 HEV ORF2 (dotted line) were analyzed daily in mouse plasma (red) and stool (black).

485